

## Monitoring and Prediction of the Urmia Lake Drying Trend Based on Time-Series Remotely Sensed Images and Artificial Neural Networks



Vahid Sadeghi

Assitant professor, Department of Geomatics Engineering, Faculty of Civil Engineering, University of Tabriz, Tabriz 5166616471, Iran

Corresponding Author Email: [v.sadeghi@tabrizu.ac.ir](mailto:v.sadeghi@tabrizu.ac.ir)

<https://doi.org/10.18280/ts.390415>

### ABSTRACT

**Received:** 23 January 2021

**Accepted:** 20 June 2022

#### **Keywords:**

*artificial neural networks, drying trend, modelling, prediction, remote sensing, Urmia Lake*

Urmia Lake, which is the second largest permanent hypersaline lake in the world, is shrinking in recent decades. Since accurate spatial information about the lake is essential to managing the current and emerging crises of the lake, this study is used Urmia Lake satellite images time-series to investigate drought trends by analyzing via Artificial Neural Networks (ANN). The proposed approach is comprising the following four steps. First, yearly time-series Landsat images (2000-2022) are corrected geometrically and radiometrically. Then, time-series images of 2000-2020 are classified into five land cover classes, including; deep water, shallow water, salt, soil, and vegetation. In the third step, ANN trained for 2000-2019 as input and tested for 2020 as an output. Finally, the trained ANN is proposed to predict the future land covers of the lake (for 2021 and 2022 years). In order to evaluate the proposed model, the predicted maps of 2021 and 2022 were compared with their corresponding ground truth maps and quantitative criteria were calculated. The overall accuracy of the prediction for 2021 and 2022 is equal to 92.75% and 90.62%, respectively, which indicates the high capability of the proposed method for modeling and predicting changes in Urmia Lake and its shores.

## 1. INTRODUCTION

In the arid and semi-arid regions, Iran does not have adequate water resources and is lower than the global average. Drought, climate fluctuations, lack of precipitation, and disorder have faced the region more and more with all kinds of water and food problems. Hence, using and drawing off from surface and subsurface waters has long been a remedy for water shortages in various sectors of agriculture, economics, industry, and drinking. On the other hand, increasing the concentration of greenhouse gases, especially carbon dioxide, caused changes in precipitation and temperature and followed by changes in some components of the hydrology cycle in recent decades [1].

Urmia Lake is the largest inland lake in Iran and the second in the world, where located between East Azerbaijan and West Azerbaijan provinces. Urmia Lake catchment area is 51800 km<sup>2</sup>, which covers about 3% of the total area of the country. In addition to that, it is the second largest permanent hypersaline lake in the world. Urmia Lake is one of the most important aquatic ecosystems in northwestern Iran, where the trend of changes in the lake surface in different climatic and socio-economic, and hydrological conditions has been various and usually decreasing. Accordingly, monitoring and modeling lake water changes and their relationship with climate change and regional hydrology are significant and necessary [2].

One of the important man-made factors in the hydrological changes of the lake is the construction of a dam in that area. In the other words, there have been a drought and dam construction projects during the past decade and there are

significant differences in lake water levels. The drying process of Urmia Lake has begun over the past three decades. After recording the highest lake level in 1995, the average lake level was reduced to 40 cm in two decades, and in September of 2014, the lake's southern portion was almost completely dried. Since the average lake depth in that area is about 6 meters, it can be estimated how much water has been lost from the southern part of the lake and its compensation is very time consuming. On the other hand, it has imposed a lot of damage to that geographical area in the environmental, socio-economic, etc. aspects [3]. From 2015 to 2022, the lake conditions improved due to increased rainfall and some arrangements by environmental activists and related working groups. In the last years, the unprecedented heat has resulted in increased evaporation from the lake's surface and led to the lake level decreasing.

Comprehensive and accurate spatial information about the lake and surrounding area is essential to managing the current and emerging crises of the lake. In recent years, different data sources, various tools, and methods have been used in water resource fields. Satellite Remote Sensing (RS) images accessibility compared to limited ground-based observations made it a cost-effective data source for water resources applications [4-11]. The various temporal and spatial resolutions of satellite images make it possible to investigate and monitor water resources phenomena, water level changes, and water resources crisis management [9].

Change modeling of water resource parameters such as water level, water surface, and water volume, is done using different algorithms and one of the most recent is the Artificial Neural Network (ANN) algorithms. Since ANN has many

capabilities such as nonlinear modeling, complex problem solving (such as Land Use/ Land Cover (LULC) changes), flexibility in modeling, and supervised and unsupervised modeling, it has been widely used in various applications, especially in the water resource fields [12-16]. Recently different ANNs have been used to model the shoreline changes in Narrabeen Coast, Australia, between 1980 and 2014 [17]. They reported that the NARNET and NARXNET have the ability to accurately estimate the shoreline positions based on the historical data available for Narrabeen Coast. In the prediction of the LULC over Mumbai (India) was conducted via multilayer perceptron ANN and Markov chain model based on multi-temporal remotely sensed images [18]. A supervised classification algorithm was applied to the remote sensing images of 1992, 2002, and 2011 to provide the historical dynamics of the LULC. Based on the modeled spatial drivers, the LULC was estimated for 2011. Zhu et al. [19] have used two machine learning models (feed forward ANN and Deep Learning) to predict monthly lake water level in Poland. The two models were employed for one month ahead forecasting of water level in 69 lakes. The evaluation results show that both the mentioned models performed generally well for estimating lake water level with only marginal differences. In a similar study, Feed Forward and Recurrent ANNs have been used to predict lake level based on long time-series hydrological data [20]. The results indicated the high capability of ANNs in predicting monthly lake water level changes. An ANN model has been used to predict water level fluctuations of Lake Van (Turkey) [13]. The results showed that the ANN model is simpler and more reliable than the conventional methods such as autoregressive moving average with exogenous input (ARMAX) and autoregressive (AR) models.

Although there have been numerous studies on predicting LULC changes using a diverse range of ANNs only a few studies have used the ANNs and time-series satellite images to predict lake surface [21, 22]. Given the capabilities of the ANN model and remote sensing data, in this study, the drying trend of Urmia Lake is investigated via analysis of time-series remotely sensed images and an ANN model. In the other words, this research tried to model and predict the lake area using time series of data obtained from RS techniques and applying the ANN methods.

## 2. DATA AND METHOD

There is a data preparation phase in modeling using satellite images. Then by classifying the data, they are used as ANN input.

### 2.1 Data

Satellite images can be acquired from different spectral bands, including optical, thermal, and microwave ranges of the electromagnetic spectrum. In this study, optical Landsat satellite images have been used from the United States Geological Survey (USGS) database to monitor and predict the drying process of Urmia Lake. The used multi-temporal Landsat satellite imageries of Urmia Lake, from 2000 to 2022 are shown in Figure 1.

The declining trend of the lake water level (blue (deep) and cyan (shallow) areas) from 2000 to 2014 is quite clear that a

very large and significant area of the lake has dried up. Then its change to an upward trend from 2014 onwards has caused the lake to get out of its moribund state.

### 2.2 Classification of time-series images using ANN

In order to classify remote sensing images as ANN input, a set of Ground Truth samples provided from the spectral library database must be used. Here, the studied area has been divided into five classes include; deep water, shallow water, salt, soil, and vegetation. Each class had to introduce a set of pixels per class. These data as known pixels need to be defined as training data for the ANN.

Each ANN consists of some nodes with weighted link connections. The main task of each node is that it receives input from its neighbor nodes to compute a final output or inputs for other nodes. In fact, nodes are related to different layers in the neural network. In the neural network, there are several layers such as input, hidden, and output layers. After receiving input and processing, the output layer shows the results. ANNs are two basic steps of training and recalling processing, which start with the import of satellite images and training data of that neural network [4, 23].

In this research, a Multi Layer Perceptron (MLP) neural network with two hidden layers is used to classify the satellite images. Back-propagation learning and gradient descent algorithm are used to train ANN. Inputs are image spectral band values for each pixel of training data, and output is corresponding to the land cover label or ground truth. As shown in Figure 2 (classification section), the ANN has six input neurons which are equal to the number of spectral bands and one output neuron which is equal to the label of the corresponding pixel in the LULC map (1: deep water, 2: shallow water, 3: salt, 4: soil and 5: vegetation). Using the trained ANN the time-series images (2000-2020) are classified and the time-series LULC maps are provided to model LULC changes in the Urmia Lake.

### 2.3 Neural network modeling of LULC changes

Based on the concepts in ANN, the future state of the lake can be predicted if the trend of previous years of the lake surface and its modeling process can be estimated as ANN output from the input parameters. For this purpose, the time-series LULC maps of 2000 through 2019 have been entered as the input of the ANN, and the LULC map of 2020 has been defined as the output so that the network should be trained.

In the following, an MLP neural network with two hidden layers is used to model LULC changes in the Urmia Lake. Inputs are the historical LULC maps (the 2000-2019 time-series LULC maps) and output is corresponding to the future land cover map (2020 LULC map in the training phase and 2021 and 2022 LULC maps in the recalling phase). As shown in Figure 2 (Modelling and Prediction section), the ANN has 20 input neurons which are equal to the number of historical LULC maps (2000-2019 time-series LULC maps), and one output neuron which is equal to the future label of the corresponding pixel. 20% of the data were used to test the neural network training rate and applied 20% for the evaluation of final results. After training the neural network with the 2000 to 2020 trend, the LULC maps of the Urmia Lake have been predicted for 2021 and 2022 years.

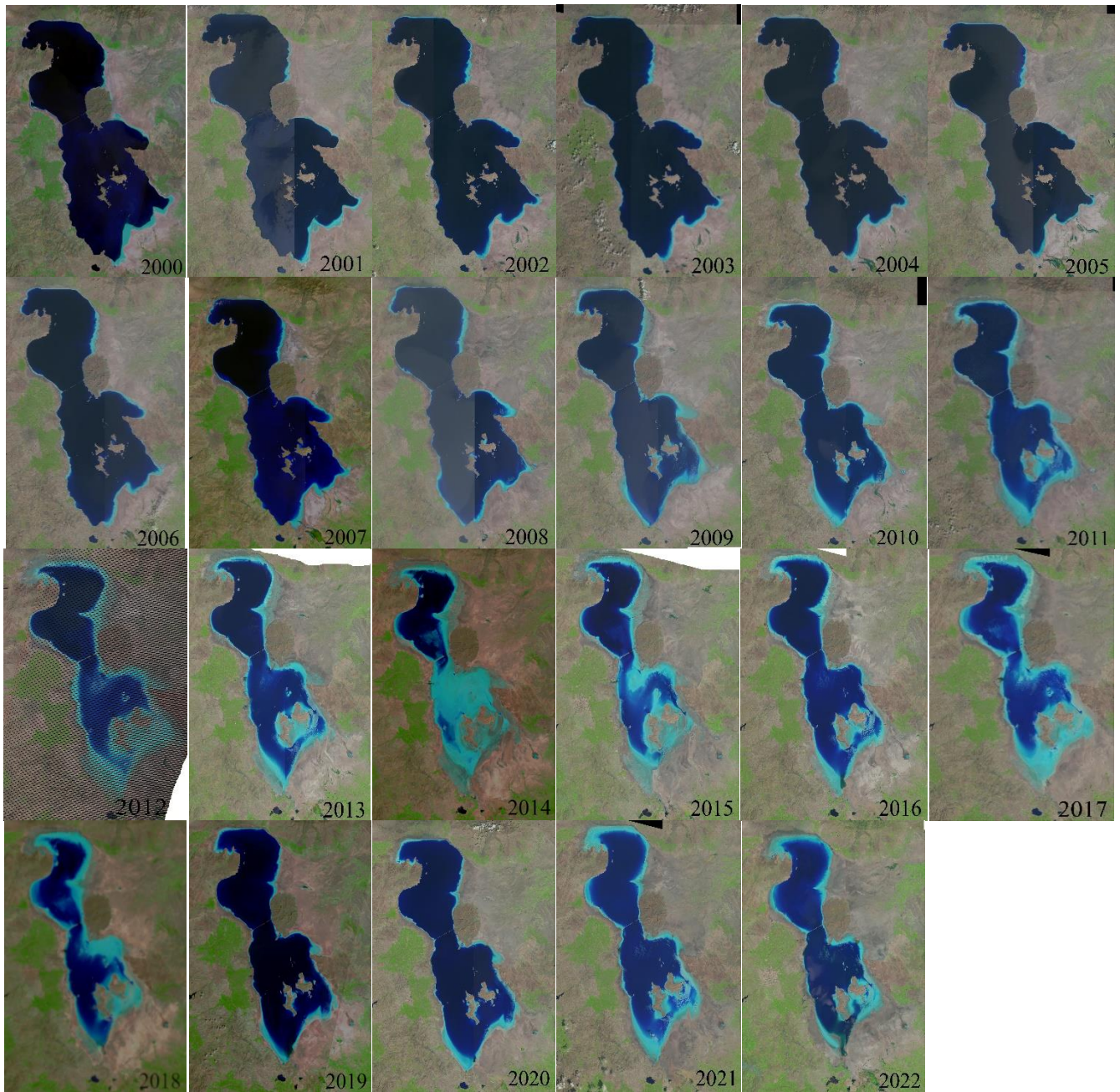


**Figure 1.** Time series Landsat satellite imageries of Urmia Lake during 2000– 2022

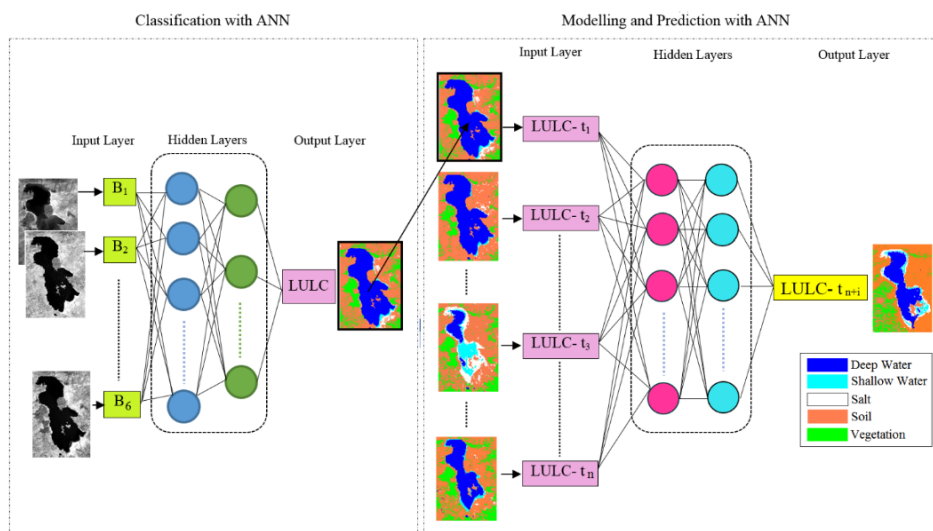


**Figure 2.** Schematic diagram of the proposed approach for LULC classification, modelling and prediction

## 2.4 Accuracy assessment of the prediction

To evaluate the proposed method, the predicted maps of 2021 and 2022 were compared with their corresponding ground truth maps and quantitative criteria were calculated using Error Matrix (Tables 1 and 2). The error matrix (confusion matrix) is a frequently used statistical tool for accuracy assessment of the classification [24]. The content of a confusion matrix is a set of values accounting for the degree of similarity between paired observations between a predicted and a reference data set (ground truth). It is a C×C squared matrix where C denotes the number of classes and the diagonal elements contain the correctly classified items and the off-diagonal elements contain the number of confusions. Different indices such as overall accuracy (OA), kappa coefficient, user's accuracy, and producer's accuracy can be extracted from the confusion matrix. The overall accuracy is the percentage of pixels correctly classified. Kappa coefficient evaluates how well the classification performed as compared to just randomly assigning values. The kappa coefficient can range from zero to one. The zero value indicated that the classification is no better than a random classification. The user's accuracy is indicative of the probability that a pixel classified in the image actually represents that category on the ground and the producer's accuracy indicates the probability of a pixel being correctly classified.

As shown in Table 1, the overall accuracy and kappa coefficient of the predicted map for 2021 are 92.75% and 0.89, respectively. In detail, the producer and user accuracy are 91.04% and 99.97% for the deep water class and 93.64% and 49.66% for the shallow water class, respectively. As is clear,

the shallow water class has been overestimated. Almost 261,519 pixels of deep water have been classified as shallow water mistakenly and therewith the user's accuracy of shallow water has been decreased to 49.66%. It is worth noting that the total number of incorrectly classified pixels is not significant compared to pixels that are correctly classified in the deep and shallow water classes and can be ignored (5,044 vs. 3,080,830, approximately 0.16%). It indicates the high ability of the model to predict the LULC for this area.

The evaluation parameters of prediction accuracy for 2022 LULC map of Urmia Lake are presented in Table 2. As indicated in Table 2, the overall accuracy and kappa coefficient of the predicted map for 2022 are 90.62% and 0.86, respectively. In detail, the producer and user accuracy are 98.39% and 94.58% for the deep water class and 84.28% and 80.74% for the shallow water class, respectively. It indicates the high ability of the model to predict the condition of the lake water. Another interpretation of the table is that the prediction results for the deep water and shallow water classes are slightly higher than the actual existence, in fact, the water class has been overestimated. In the other words, about 105,943 pixels of the salt class were mistakenly classified in the deep water class and 78,352 pixels of the salt class in the shallow water class, increasing the number of water class pixels. Also from the two soil and vegetation classes, approximately 742 pixels (28 + 462 + 19 + 233 = 742) were incorrectly categorized in the deep water and shallow water classes. Remarkably, the total number of incorrectly classified pixels is not significant compared to pixels that are correctly classified in the water class (shallow and deep) (185,037 vs. 2,664,285, approximately 7%) and can be ignored.

**Table 1.** Error matrix and accuracy assessment report of the predicted 2021 land cover map

		True class					Total	User's Accuracy (%)
		Deep Water	Shallow Water	Salt	Soil	Vegetation		
Predicted class	Deep Water	2,817,911	773	0	2	0	2,818,686	99.97
	Shallow Water	261,519	262,919	4,213	791	38	529,480	49.66
	Salt	12,034	17,075	313,478	73,757	6,292	422,636	74.17
	Soil	3,905	15	89	5,000,046	39,650	5,043,705	99.13
	Vegetation	33	0	0	409,239	1,607,018	2,016,290	79.70
	Total	3,095,402	280,782	317,780	5,483,835	1,652,998		Overall Accuracy=92.75%
Producer's Accuracy (%)		91.04	93.64	98.65	91.18	97.22		Kappa Coefficient = 0.89

**Table 2.** Error matrix and accuracy assessment report of the predicted 2022 land cover map

		True class					Total	User's Accuracy (%)
		Deep Water	Shallow Water	Salt	Soil	Vegetation		
Predicted class	Deep Water	2,331,553	27,504	105,943	28	19	2,465,047	94.58
	Shallow Water	306	332,732	78,352	462	233	412,085	80.74
	Salt	13,427	32,659	528,248	48,634	5	622,973	84.79
	Soil	23,654	1,876	47,539	5,041,475	42,347	5,156,891	97.76
	Vegetation	805	4	169	649,711	1,508,979	2,159,668	69.87
	Total	2,369,745	394,775	760,251	5,740,310	1,551,583		Overall Accuracy= 90.62%
Producer's Accuracy (%)		98.39	84.28	69.48	87.83	97.25		Kappa Coefficient = 0.86

## 3. CONCLUSIONS

Detection and prediction of LULC change of water bodies are necessary to take care of an ecosystem, especially in areas with rapid and often unplanned changes in developing countries such as Iran. There has been numerous research on predicting LULC changes using ANNs, only a few studies have used the ANNs and time-series satellite images to predict Lake surface. Using the ANN model and satellite image data,

the water resource change in Urmia Lake has been investigated in this research.

The proposed method is totally comprised of four steps. Yearly time-series Landsat satellite images (2000-2022) are corrected geometrically and radiometrically in the first step. Secondly, they are classified into five land covers using the MLP neural network. In the third phase, another MLP neural network is trained for 2000-2019 as input and tested for 2020 as an output. In the last step, the trained ANN is recalled to

predict the future land covers of the Urmia Lake for 2021 and 2022 years. In order to assess the proposed model, the predicted maps of 2021 and 2022 were compared with their corresponding ground truth maps and quantitative criteria were calculated. The overall accuracy and kappa coefficient of the prediction for 2021 are equal to 92.75% and 0.89, respectively, and for 2022 are equal to 90.62% and 0.86, respectively. It means that the proposed method is useful and applicable for modeling and predicting changes in Urmia Lake and its shores.

The obtained result shows that the Urmia Lake drying trend has increased noticeably in recent decades. It led to the creation of large salinized land areas in the dried lake bed and its surrounding area. In addition, the trend of changes in Urmia Lake from 2000 to 2014 witnessed a noticeable decrease in water and shallow water regions and in the last 8 years, the amount of water and shallow regions has increased gradually with slight fluctuations. This increase, which was due to changes in weather and rainfall conditions, was not enough to compensate for the losses and shortages.

## REFERENCES

- [1] Madani, K. (2014). Water management in Iran: What is causing the looming crisis? *Journal of Environmental Studies and Sciences*, 4(4): 315-328. <http://dx.doi.org/10.1007/s13412-014-0182-z>
- [2] Tourian, M.J, Elmi, O., Chen, Q., Devaraju, B., Roohi, S., Sneeuw, N. (2015). A spaceborne multisensor approach to monitor the desiccation of Lake Urmia in Iran. *Remote Sensing of Environment*, 156: 349-360. <http://dx.doi.org/10.1016/j.rse.2014.10.006>
- [3] Delju, A.H., Ceylan, A., Piguët, E., Rebetez, M. (2013). Observed climate variability and change in Urmia Lake Basin, Iran. *Theoretical and Applied Climatology*, 111(1): 285-296. <http://dx.doi.org/10.1007/s00704-012-0651-9>
- [4] Carrera, E. (1995). Image classification using artificial neural networks. *International Conference on Education, Practice, and Promotion on Computational Methods in Engineering Using Small Computers (EPMESC V)*.
- [5] Chawla, I., Karthikeyan, L., Mishra, A.K. (2020). A review of remote sensing applications for water security: Quantity, quality, and extremes. *Journal of Hydrology*, 585: 124826. <http://dx.doi.org/10.1016/j.jhydrol.2020.124826>
- [6] Farahmand, N., Sadeghi, V. (2020). Estimating soil salinity in the dried lake bed of Urmia Lake using optical sentinel-2 images and nonlinear regression models. *Journal of the Indian Society of Remote Sensing*, 48: 675-687. <http://dx.doi.org/10.1007/s12524-019-01100-8>
- [7] Sadeghi, V., Farnood Ahmadi, F., Ebadi, H. (2016). Design and implementation of an expert system for updating thematic maps using satellite imagery (case study: Changes of Lake Urmia). *Arabian Journal of Geosciences*, 9(4): 257. <http://dx.doi.org/10.1007/s12517-015-2301-x>
- [8] Sadeghi, V., Farnood Ahmadi, F., Ebadi, H. (2018). A new fuzzy measurement approach for automatic change detection using remotely sensed images. *Measurement*, 127: 1-14. <http://dx.doi.org/10.1016/j.measurement.2018.05.097>
- [9] Van Dijk, A., Renzullo, L., Rodell, M. (2011). Use of gravity recovery and climate experiment terrestrial water storage retrievals to evaluate model estimates by the Australian water resources assessment system. *Water Resources Research*, 47: 1-12. <http://dx.doi.org/10.1029/2011WR010714>.
- [10] Xiao, X., Xie, J., Niu, J., Cao, W. (2020). A novel image fusion method for water body extraction based on optimal band combination. *Traitement du Signal*, 37(2): 195-207. <http://dx.doi.org/10.18280/ts.370205>
- [11] Zhang, J., Feng, M., Wang, Y. (2020). Automatic segmentation of remote sensing images on water bodies based on image enhancement. *Traitement du Signal*, 37(6): 1037-1043. <http://dx.doi.org/10.18280/ts.370616>
- [12] Agarwal, A., Singh, R. (2004). Runoff modelling through back propagation artificial neural network with variable rainfall-runoff data. *Water Resources Management*, 18(3): 285-300. <http://dx.doi.org/10.1023/B:WARM.0000043134.76163.b9>
- [13] Altunkaynak, A. (2007). Forecasting surface water level fluctuations of Lake Van by artificial neural networks. *Water Resources Management*, 21(2): 399-408. <http://dx.doi.org/10.1007/s11269-006-9022-6>
- [14] Cancelliere, A., Giuliano, G., Ancarani, A., Rossi, G. (2002). A neural networks approach for deriving irrigation reservoir operating rules. *Water Resources Management*, 16(1): 71-88. <https://doi.org/10.1023/A:1015563820136>
- [15] Jain, A., Varshney, A.K., Joshi, U.C. (2001). Short-term water demand forecast modelling at IIT Kanpur using artificial neural networks. *Water Resources Management*, 15(5): 299-321. <https://doi.org/10.1023/A:1014415503476>
- [16] Kumar, D.N., Raju K.S., Sathish, T. (2004). River flow forecasting using recurrent neural networks. *Water Resources Management*, 18(2): 143-161. <https://doi.org/10.1023/B:WARM.0000024727.94701.12>
- [17] Zeinali, S., Dehghani, M., Talebbeydokhti, N. (2021). Artificial neural network for the prediction of shoreline changes in Narrabeen, Australia. *Applied Ocean Research*, 107: 102362. <http://dx.doi.org/10.1016/j.apor.2020.102362>
- [18] Vinayak, B., Lee, H.S., Gedom, S. (2021). Prediction of land use and land cover changes in Mumbai City, India, using remote sensing data and a multilayer perceptron neural network-based Markov chain model. *Sustainability*, 13(2): 471. <http://dx.doi.org/10.3390/su13020471>
- [19] Zhu, S., Hrnjica, B., Ptak, M., Choiński, A., Sivakumar, B. (2020). Forecasting of water level in multiple temperate lakes using machine learning models. *Journal of Hydrology*, 585: 124819. <http://dx.doi.org/10.1016/j.jhydrol.2020.124819>
- [20] Hrnjica, B., Bonacci, O. (2019). Lake level prediction using feed forward and recurrent neural networks. *Water Resources Management*, 33(7): 2471-2484. <http://dx.doi.org/10.1007/s11269-019-02255-2>
- [21] Imani, M., You, R.J, Kuo, C.Y. (2014). Caspian Sea level prediction using satellite altimetry by artificial neural networks. *International Journal of Environmental Science and Technology*, 11(4): 1035-1042. <http://dx.doi.org/10.1007/s13762-013-0287-z>
- [22] Sadeghi, V., Etemadfar, H., Naeimi, Y. (2022). Design

- of water level-surface models for Urmia Lake based on ground and space observations. Iranian Water Researches Journal, 15(43).
- [23] Patterson, D.W. (1998). Artificial Neural Networks: Theory and Applications. Prentice Hall PTR.
- [24] Congalton, R.G. (1991). A review of assessing the accuracy of classifications of remotely sensed data. Remote Sensing of Environment, 37(1): 35-46. [http://dx.doi.org/10.1016/0034-4257\(91\)90048-B](http://dx.doi.org/10.1016/0034-4257(91)90048-B)